

HD-A137 842

MECHANICAL AND PHYSICAL PROPERTIES OF POLY(VINYLIDENE  
FLUORIDE) AT HIGH P. (U) RUTGERS - THE STATE UNIV  
PISCATAWAY NJ HIGH PRESSURE MATERIAL... K D PAE ET AL.

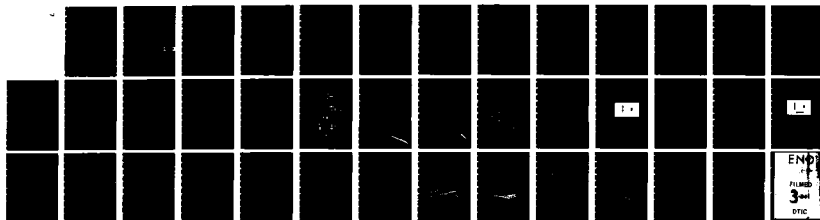
1/1

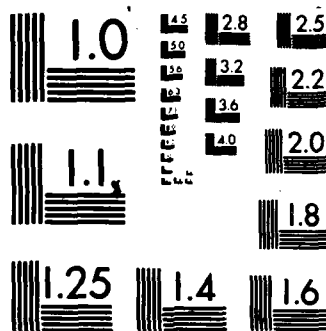
UNCLASSIFIED

31 JAN 84 TR-25 N00014-75-C-0540

F/G 11/9

NL





MICROCOPY RESOLUTION TEST CHART  
NATIONAL BUREAU OF STANDARDS-1963-A

AD A137842

DTIC FILE COPY

SECURITY CLASSIFICATION OF THIS PAGE (When Data Entered)

REPORT DOCUMENTATION PAGE		READ INSTRUCTIONS BEFORE COMPLETING FORM
1. REPORT NUMBER Technical Report # 25	2. GOVT ACCESSION NO.	3. RECIPIENT'S CATALOG NUMBER
4. TITLE (and Subtitle) MECHANICAL AND PHYSICAL PROPERTIES OF POLY(VINYLDENE FLUORIDE) AT HIGH PRESSURES AND TEMPERATURES.		5. TYPE OF REPORT & PERIOD COVERED Technical Report Interim
		6. PERFORMING ORG. REPORT NUMBER
7. AUTHOR(s) K. D. Pae, K. Vijayan, R. W. Renfree, K. T. Chung, J. I. Scheinbeim, and B. A. Newman		8. CONTRACT OR GRANT NUMBER(s) N00014-75-C-0540
9. PERFORMING ORGANIZATION NAME AND ADDRESS ✓ High Pressure Materials Research Laboratory and Department of Mechanics and Materials Science, Rutgers University, P.O. Box 909, Piscataway, NJ		10. PROGRAM ELEMENT, PROJECT, TASK AREA & WORK UNIT NUMBERS NR 356-564
11. CONTROLLING OFFICE NAME AND ADDRESS Office of Naval Research (Code 472) Arlington, VA 22217		12. REPORT DATE
		13. NUMBER OF PAGES
14. MONITORING AGENCY NAME & ADDRESS (if different from Controlling Office)		15. SECURITY CLASS. (of this report)
		15a. DECLASSIFICATION/DOWNGRADING SCHEDULE
16. DISTRIBUTION STATEMENT (of this Report) Approved for public release; distribution unlimited. Reproduction in whole or in part is permitted for any purpose of the United States Government.		
17. DISTRIBUTION STATEMENT (of the abstract entered in Block 20, if different from Report)		
18. SUPPLEMENTARY NOTES		
19. KEY WORDS (Continue on reverse side if necessary and identify by block number) Poly(vinylidene fluoride), Piezoelectricity, pyroelectricity high pressure effects, Young's modulus, yield strengths, thermal expansion, compressibility glass transition		
20. ABSTRACT (Continue on reverse side if necessary and identify by block number) Stress-strain behavior in tension and compression at various pressures, Pressure-Volume-Temperature (PVT) relations, and the pressure dependency of transitional behavior, by dielectric technique, of Phase I and Phase II poly(vinylidene fluoride) (PVDF) have been determined. The result obtained are used in analyzing the complex behavior of piezoelectric and pyroelectric properties of the material at high pressures and temperatures. The Young's modulus (E) of Phase II PVDF increases, at room temperature, monotonically.		

DTIC  
ELECTE  
S FEB 14 1984 D  
D

## 20. ABSTRACT (continued)

but nonlinearly, with increasing pressure as long as the amorphous material is in the rubbery state. It then takes a step-jump at  $P_g$  (5 Kbars) and continues to increase with pressure. However, the yield strength in both tension and compression is observed to be linear functions of pressure. PVT measurements clearly show the glass transition temperature ( $T_g$ ) at  $-50^\circ\text{C}$  and the crystal transition ( $T_c$ ) at  $22^\circ\text{C}$  at atmospheric pressure. The  $T_g$  of both unoriented and oriented Phase I PVDF increase, in most part, linearly with increasing pressure, except at low pressures where the increase is parabolic. The linear compressibility of unoriented Phase I PVDF at room temperature is a nonlinearly decreasing function of pressure, varying from  $6.8 \times 10^{-6} \text{ cm}^2/\text{N}$  at atmospheric pressure to  $2.7 \times 10^{-6} \text{ cm}^2/\text{N}$  at 6 Kbars. The linear compressibility of oriented Phase I PVDF in the transverse direction is much greater than that in the machine direction. The difference in the linear compressibilities diminishes with increasing pressure. A comparison between the minimum points in the plots of  $d_p$  and  $P_y$  versus temperature and the  $T_g$  at various pressures shows that, even though different molecular motions are responsible for these activities, there appears to be a common influence by hydrostatic pressure.

Accession For	
DTIC TAB	<input checked="checked" type="checkbox"/>
Unannounced	<input type="checkbox"/>
Justification	
By	
Distribution/	
Availability Codes	
Dist	Avail and/or Special
A/1	



OFFICE OF NAVAL RESEARCH

Contract N00014-75-C-0540

Task No. NR 356-564

TECHNICAL REPORT No. 25

MECHANICAL AND PHYSICAL PROPERTIES  
OF POLY(VINYLDENE FLUORIDE) AT  
HIGH PRESSURES AND TEMPERATURES

by

K. D. Pae, K. Vijayan, R. W. Renfree, K. T. Chung,  
J. I. Scheinbeim, and B. A. Newman

Prepared for Publication

In the

Ferroelectrics

High Pressure Materials Research Laboratory  
Department of Mechanics and Materials Science  
College of Engineering  
Rutgers University  
P.O. Box 909  
Piscataway, New Jersey 08854

January 31, 1984

Reproduction in whole or in part is permitted for any  
purpose of the United States Government.

This document has been approved for public release  
and sale; its distribution is unlimited.

MECHANICAL AND PHYSICAL PROPERTIES OF  
POLY(VINYLDENE FLUORIDE) AT HIGH PRESSURES AND TEMPERATURES

by

K. D. Pae, K. Vijayan, R. W. Renfree, K. T. Chung,

J. I. Scheinbeim and B. A. Newman

High Pressure Materials Research Laboratory

Rutgers University

P.O.Box 909, Piscataway, New Jersey 08854

I. INTRODUCTION

Stress-strain behavior in tension and compression, Pressure-Volume-Temperature(PVT) relations, especially bulk and linear thermal expansion and compressibility, and the transition temperatures and their pressure dependencies of poly(vinylidene fluoride) (PVDF) have been determined as functions of hydrostatic pressure and temperature.

The stress-strain behavior of PVDF at high pressures represents the basic mechanical characteristics, encompassing elastic and plastic ranges, such as the modulus of elasticity, the yield strength, the ductility, and the fracture modes. These characteristics are indispensable in understanding and application of PVDF at atmospheric and high pressure environment.

PVT relationships are essential in establishing equations of state(1,2) and the results of the measurements, namely the

compressibility and thermal expansion data are needed in calculating theoretical values of piezoelectric and pyroelectric constants(3,4). These quantities on bulk samples of Phase II PVDF, film samples of unoriented Phase I PVDF, which was obtained by the "p-jump"(pressure quench) technique, and the "Piezofilm" (Kureha) samples in the direction of and perpendicular to the machine direction have been determined at various pressures and temperatures. The linear and bulk compressibility measurement provides also locations of various transition temperatures and their pressure dependencies.

## II. EXPERIMENTAL

The stress-strain tests in tension and compression at high pressures have been carried out in an apparatus shown in Fig. 1. The apparatus is capable of containing pressures to 10 Kbars and maintains constant pressure during loading and unloading process. The pressure transmitting fluid is a high purity silicon oil with low viscosity(5-cs). Load-deformation curves were obtained and converted to nominal(or engineering) stress-strain curves as shown in Fig. 2 and 3. The loading process is assumed isothermal, quasi-static (the rate of loading = 0.02 in/in/min), and independent of time(no creep and relaxation).

The bulk compressibility of melt crystallized sample of Phase II PVDF in a form of circular cylinder and the linear

compressibility of thin films, which were rolled into hollow circular cylinders were carried out in a high pressure vessel. Temperature of the vessel is controlled by an internal furnace and a cooling coil wound around the cylinder, through which liquid nitrogen is passed. The range of temperature employed for this series of experiments is approximately from  $-100^{\circ}\text{C}$  to  $+100^{\circ}\text{C}$ . Measurements were taken during either or both cooling and heating cycle at a rate of about  $1^{\circ}\text{C}/\text{min}$ . A linear variable differential transformer (LVDT) is used to detect changes in linear dimension of the sample cylinders in the axial direction (Fig. 4).

The molecular transition temperatures; namely the  $T_g$  and  $T_c$ , for these various samples were determined from the plots of the specific volume versus temperature at various pressures as shown in Fig. 5, 13, 19, and 22.

### III. MATERIAL

For the stress-strain experiments, samples were compression-molded from PennWalt Kynar pellets and machined into circular cylinders. These samples were crystallized into Phase II material. The tensile samples have the gage section of 0.25 inch diameter and 1.0 inch length with raised and threaded ends for gripping (Fig. 6). The compressive samples have the dimensions of 0.50 in. diameter and 1.0 inch length (Fig. 6).

For Pressure-Volume-Temperature studies, bulk samples were



prepared by exactly the same way the samples for the stress-strain tests were made. Their dimensions are 0.25 inch diameter by 1.0 inch long. The unoriented Phase I material was prepared by the "p-jump" technique which has been fully described elsewhere(5,6). To briefly comment on it; first, thin films of PVDF were recrystallized in a platten press at 210°C to remove previous thermal and mechanical history. Secondly, these films, which were then sandwiched between two aluminum foils, were heated to the melting point in a high pressure DTA cell under 1 Kbar and then pressure raised to 7 Kbars within a short period of time. Temperature is then lowered to room temperature and pressure removed. The Piezofilms were purchased from Kureha chemical Company of Japan.

#### IV. RESULTS

##### 4.1 Stress-Strain Behavior

The compressive stress-strain curves, obtained under various pressures indicated and at room temperature, are shown in Fig. 2. Each curve shows a linear elastic region, which is the measure of the stiffness, followed by a broad non-linear deformation, within which yielding occurs. No stress-induced softening, as observed in other polymers(7,8), has been observed in PVDF. Linear plastic deformation follows until the test is terminated.

In Fig. 7, the Young's modulus(E), which is obtained from the initial slope of the stress-strain curves(Fig. 2), is

plotted against applied hydrostatic pressure. The modulus  $E$  increases with increasing pressure in a non-linear fashion up to 5 Kbars. It then jumps to a new value at 6 Kbars ( $E = 3.24 \times 10^5$  psi) which is a step higher than that at 5 Kbars ( $E = 2.44 \times 10^5$  psi). It proceeds to increase to a new value at 7 Kbars ( $E = 3.40 \times 10^5$  psi). In all,  $E$  increases 3.33 times the initial value at atmospheric pressure ( $E = 1.02 \times 10^5$  psi). This step-jump in  $E$  appears to be associated with the glass transition temperature ( $T_g$ ) which is being shifted to room temperature by applied hydrostatic pressure. In fact, as will be discussed in the following with regard to the change in specific volume as a function of temperature, the  $T_g$  shifts from  $-50^\circ\text{C}$  to room temperature by about 5 Kbar pressure. In other words, the glass transition pressure ( $P_g$ ) for Phase II PVDF is situated near 5 Kbars.

The compressive yield strength, determined by 2 % off-set method, is plotted against applied hydrostatic pressure in Fig. 8. The yield strength is a linear function of pressure but appears to be not sensitive to the presence of the  $P_g$  at 5 Kbars.

Fig. 3 shows the tensile stress-strain curves of Phase II PVDF under various pressures indicated at room temperature. Each stress-strain curve contains a linear elastic region initiated from the origin, followed by a broad non-linear elastic region. The samples then undergo yielding, accompanied by

necking. Fracture then occurs in most samples within the necked region of the samples. Consequently, the cold-drawing is limited. This happens at all pressures. The tensile yield stress is plotted against applied hydrostatic pressure in Fig. 8 along with the compressive yield stress. The tensile yield stress also increases linearly with pressure.

Typical deformed samples, showing modes of deformation, are pictured in Fig. 9. The compressive sample deformed into a barrel shape from a right circular cylinder. The tensile sample shows necking and a shear fracture in the neck.

#### 4.2 PVT Studies of Unoriented Phase I Material

Figure 10 shows a plot of linear dimension versus  $P$  at room temperature for unoriented Phase I films. The open circles are the actual data points and the solid line is a polynomial fit of the form,

$$L = A + BP + CP^2 + DP^3 \quad (1)$$

where  $P$  is the applied hydrostatic pressure and the coefficients  $A$ ,  $B$ ,  $C$ , and  $D$  assume the following values:

$$A = 2.540$$

$$B = -1.733 \times 10^{-2}$$

$$C = 1.605 \times 10^{-3}$$

$$D = -1.385 \times 10^{-4}$$

The linear compressibility ( $\beta_L$ ) of the material is then calculated by

$$\beta_L = (1/L) (\partial L / \partial P) \quad (2)$$

which is shown in Fig. 11. The linear compressibility and the bulk compressibility, which is merely  $3\beta_L$ , increase rapidly at lower pressures but appear to stabilize at higher pressures. In fact, the second derivative of Eq. 1 clearly indicates that the inflection point occurs at 5 Kbars. This pressure is assigned, therefore, the glass transition pressure ( $P_g = 5$  Kbars). The lattice bulk compressibility of Phase I and II have been determined earlier in this laboratory(9) and by Tanaka, Takayama, Okamoto, and Takemura(2).

In Fig. 12 is a plot of linear dimension(L) against temperature(T) at atmospheric pressure. The temperature was varied at a rate of  $1.5^\circ\text{C}$  from  $-90^\circ\text{C}$  to  $+60^\circ\text{C}$ . The open circles are the experimental data and the solid line is the computer fit by a polynomial. To determine the thermal expansion coefficient( $\alpha$ ) at various temperatures, the slope of the actual data of the L versus T is taken by means of a discrete a three point average method and the results are shown in Fig. 13. The figure shows two sharp breaks in the slope near  $-50^\circ\text{C}$  and  $22^\circ\text{C}$ . These temperatures reflect the glass transition temperature( $T_g$ ) and the crystal transition( $T_c$ ).

#### 4.3 PVT Studies on Uniaxially Oriented Material(Piezofilm)

The linear compressibility of uniaxially oriented Piezofilm in the machine and in the transverse directions, together with that of unoriented Phase I material, is shown as a function of pressure in Fig. 14. As expected, the compressibility in the transverse direction is much greater than that in the machine direction since the transverse direction is composed of van der Waal's bonding while the machine direction should be composed mainly of covalent bonds of the oriented molecules.

In Fig. 15, bulk compressibility of the oriented and unoriented PVDF are shown as a function of pressure. The bulk compressibilities are calculated by,

$$\text{for unoriented, } \beta_v = 3 \times \beta_L \quad (3)$$

$$\text{for oriented, } \beta_v = \beta_{\parallel} + 1.5\beta_{\perp} \quad (4)$$

where an assumption is made that the compressibility in the thickness direction is 1/2 that in the perpendicular direction. The unoriented sample is more compressible than the oriented sample at all pressures including at atmospheric pressure. The difference in the compressibility between the unoriented and oriented samples decreases with increasing pressure as one might expect.

## V. DISCUSSION

Young's modulus of polymeric materials has been found to be sensitive to superposed hydrostatic pressure(10) and the pressure dependency has been predicted by the finite deformation theory of

elasticity(11) as

$$E(P) = E(0) + mP \quad (5)$$

where  $m = 2(5 - 4\nu)(1 - \nu)$ .  $\nu$  is the Poisson's ratio at atmospheric pressure. If  $\nu = 0.45$  is assumed for the range where the amorphous region is rubbery,  $m = 3.63$  and this plot is incorporated in Fig. 7. In the case of PVDF, the increase of  $E$  below  $P_g$  is nonlinear.  $E$  undergoes a step change to a new higher value at  $P_g$  and appears then to increase linearly above  $P_g$  where the amorphous region is in glassy state. The step jump of  $E$  at  $P_g$  for PVDF is more dramatic than other crystalline polymers, such as polyethylene and polypropylene for which only changes in slope of  $E$ . vs.  $P$  curve occurs. The jump is, however, not surprising in view of the fact that the PVDF samples contained approximately 50 % amorphous material while polyethylene and polypropylene samples contain less than 15 % amorphous material. Moreover, 100 % amorphous materials normally undergoes step increase at  $P_g$  in the amount on the order of several decades(12). The average increase of  $T_g$  from  $-50^\circ\text{C}$  to  $20^\circ\text{C}$  is about  $14^\circ\text{C/Kbar}$  for PVDF as compared to  $17^\circ\text{C}/1000 \text{ atm}$  for PVC,  $20^\circ\text{C}/1000 \text{ atm}$  for PVA, and  $14^\circ\text{C}/1000 \text{ atm}$  for poly(propylene oxide)(13).

The pressure dependency of the yield strength in both compression and tension is linear. While Young's modulus  $E$  undergoes a step jump at  $P_g$ , the yield strength of the material does not. This may be because the yielding involves longer range molecular rearrangements than that for  $E$ , during which sufficient

free volume is created to allow  $T_g$  to be lowered. The ratio of  $E$  to compressive yield strength appears to be about the same ( $\sim 200$ ) in both below and above  $P_g$ . The effects of the change of the mechanical properties, especially Young's modulus, on the piezoelectric and pyroelectric properties at high pressures do not appear readily recognizable.

However, the effects of  $T_g$ ,  $T_c$ , and/or  $dT_g/dP$ ,  $dT_c/dP$  on the piezoelectric and pyroelectric properties of PVDF at high pressures were found to be very significant. These results, therefore, supports the concept that the coupling between crystalline and amorphous phases does influence piezoelectric and pyroelectric properties of PVDF(14-17). In Fig. 17 and 18 are the plots of hydrostatic piezoelectric constant( $d_p$ ) and pyroelectric constant( $P_y$ ) respectively versus temperature at various pressures for unoriented phase I PVDF. The temperature for the minimum peak value(i.e.  $-70^\circ\text{C}$  for  $d_p$  at atmospheric pressure and  $-60^\circ\text{C}$  for  $P_y$  at atmospheric pressure) in Fig. 17 and Fig. 18 shifts to higher value with increasing pressure. When this shift is compared with the pressure induced shift of glass transition temperature (or  $\alpha$ -transition of dielectric loss peak), it was found that their shifts are comparable from overall point of view as shown in Fig. 19, considering the fact that different molecular mechanisms are involved in each of the electrical behaviors.

For uniaxially oriented films of PVDF,  $d_p$  and  $P_y$  versus temperature at various pressures are shown in Fig. 20 and 21,

respectively. Again, when minimum points are plotted against pressure, together with  $T_g$ , their pressure induced shifts are relatively close to each other (Fig. 22).



## REFERENCES

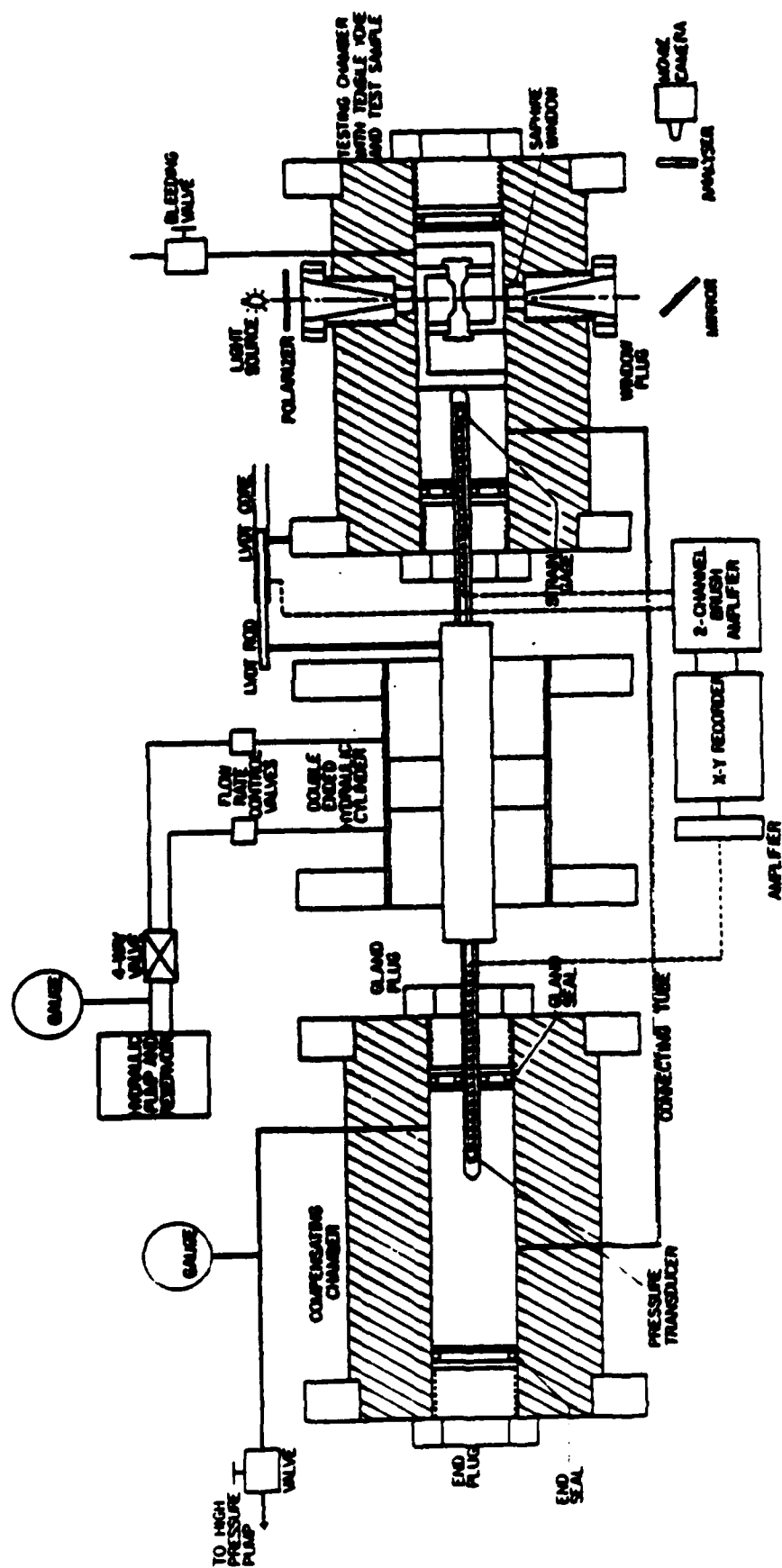
1. O. Olabisi and R. Simha, J. Appl. Polym. Sci, 21, 149(1977).
2. H. Tanaka, K. Takayama, T. Okamoto, and T. Takemura, Polym. J., 14, 719(1982).
3. M. G. Broadhurst, G. T. Davis, J. E. McKinney and R. E. Collins, J. Appl. Phys., 49, 4992(1978).
4. G. T. Davis, J. E. McKinney, M. G. Broadhurst and S. C. Roth, J. Appl. Phys., 49, 4998(1978).
5. J. Scheinbeim, C. Nakafuku, B. A. Newman and K. D. Pae, J. Appl. Phys., 50, 4399(1979).
6. K. D. Pae, B. A. Newman and J. I. Scheinbeim, U. S. Patent No. 4,349,502, September, 1982.
7. K. D. Pae and J. A. Sauer, Engineering Solids under Pressure, Ed. H. Ll. D. Pugh, Inst. Mech. Eng., London, 1971.
8. J. A. Sauer, S. K. Bhateja and K. D. Pae, Third Inter-American Conf. Mat. Tech., Rio de Janeiro, S. W. Res. Inst., San Antonio, 1972, p. 486.
9. B. A. Newman, C. H. Yoon and K. D. Pae, J. Mat. Sci., 14, 2391 (1979).
10. K. D. Pae and S. K. Bhateja, J. Macromol. Sci., Rev. Macromol. Chem., C13, 1(1975).
11. F. Birch, J. Appl. Phys., 9, 4(1938).
12. D. L. Questad, K. D. Pae, B. A. Newman and J. I. Scheinbeim, J. Appl. Phys., 51, 5100(1980).
13. J. D. Ferry, Viscoelastic Prop. Polym., 3rd Ed., Wiley, New York, 1982.
14. H. Ohigashi, J. Appl. Phys., 47, 949(1976).
15. M. Oshiki and E. Fukada, Jpn. J. Appl. Phys., 15, 43(1976).
16. P. Buckman, Ferroelectrics, 5, 39(1973).
17. H. Burkard and G. Pfister, J. Appl. Phys., 45, 3360(1974).

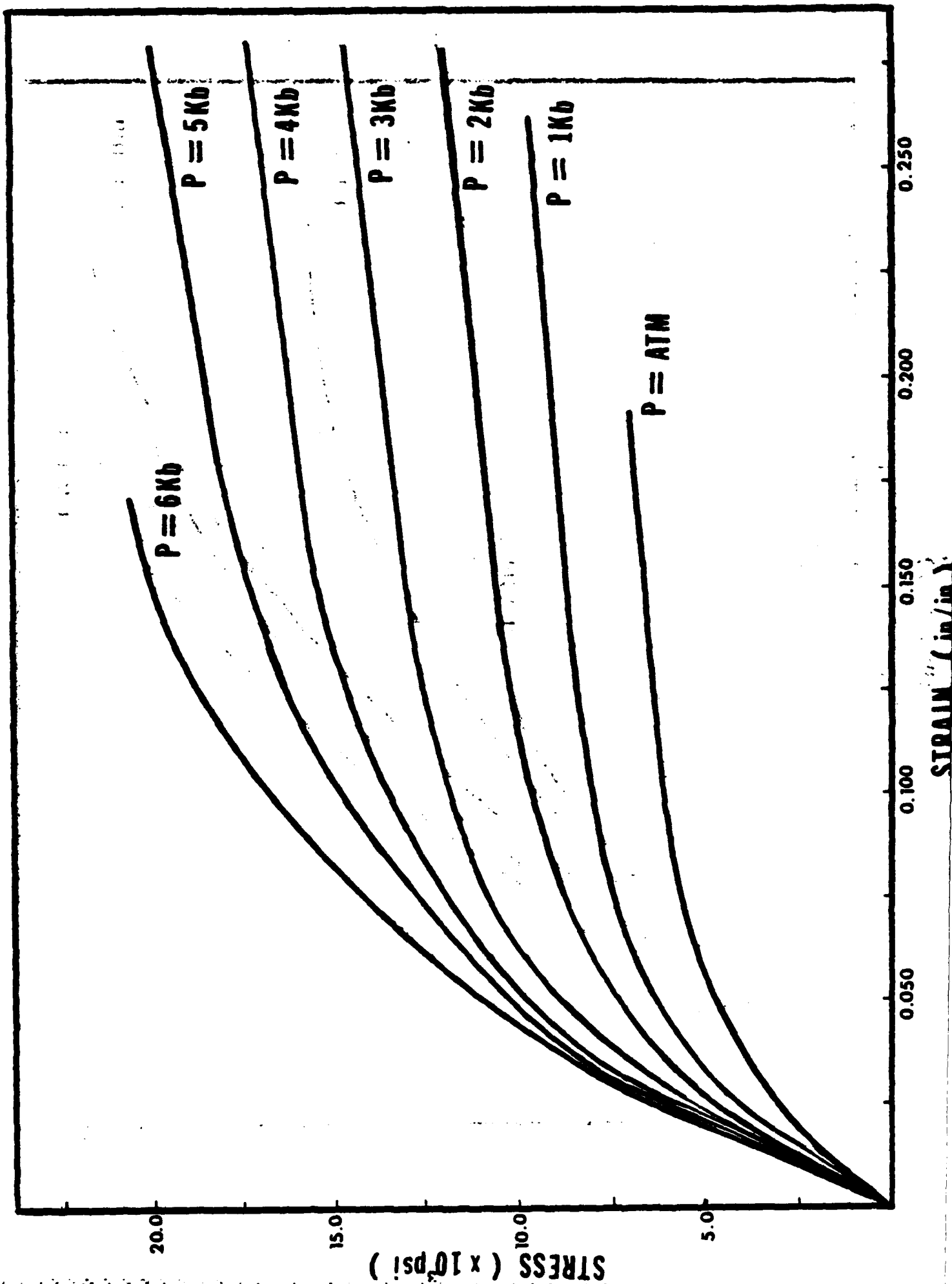
#### ACKNOWLEDGEMENT

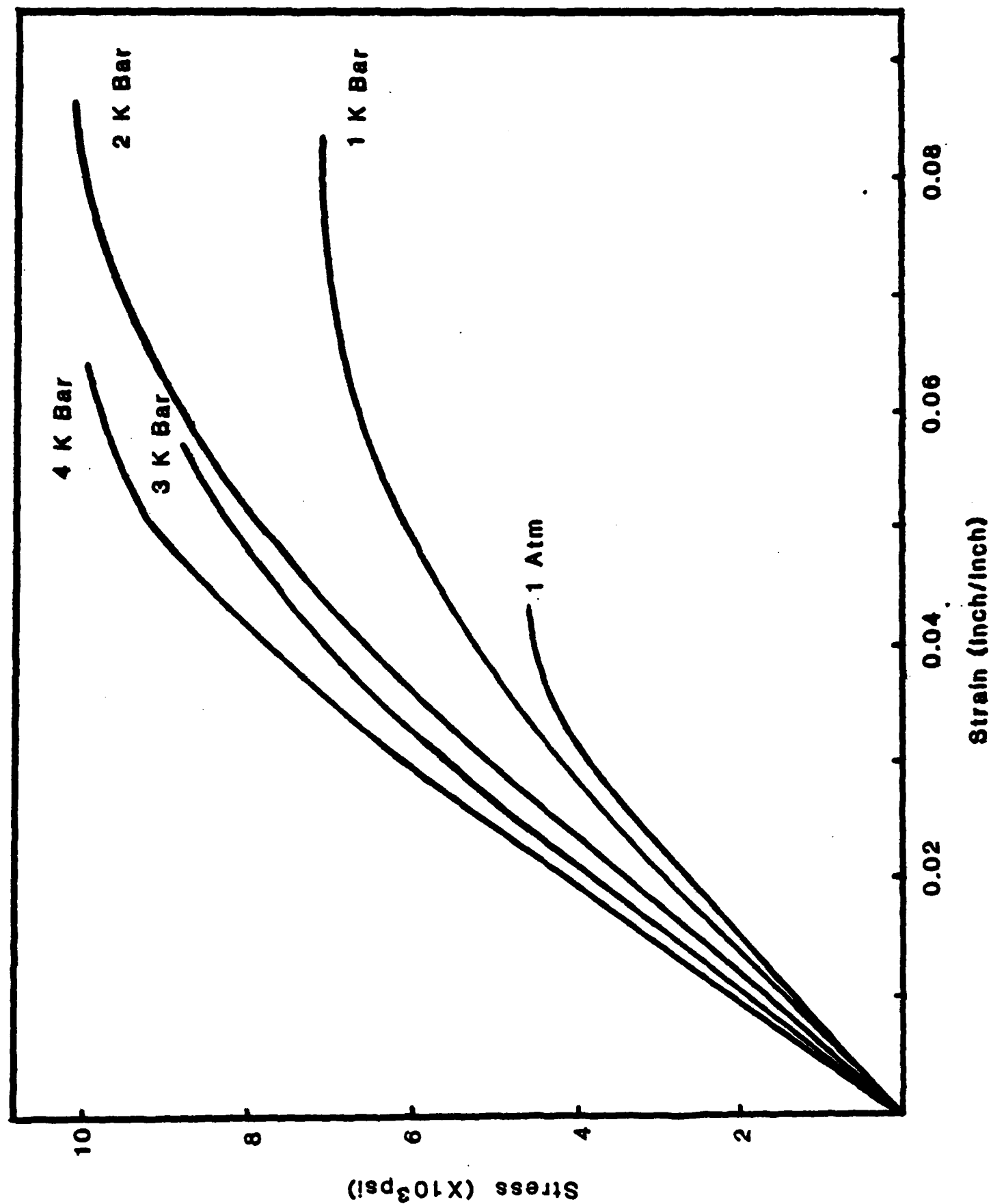
The authors gratefully acknowledge the financial support of the Office of Naval Research (Contract No. 00014-75-C-0540) for these studies.

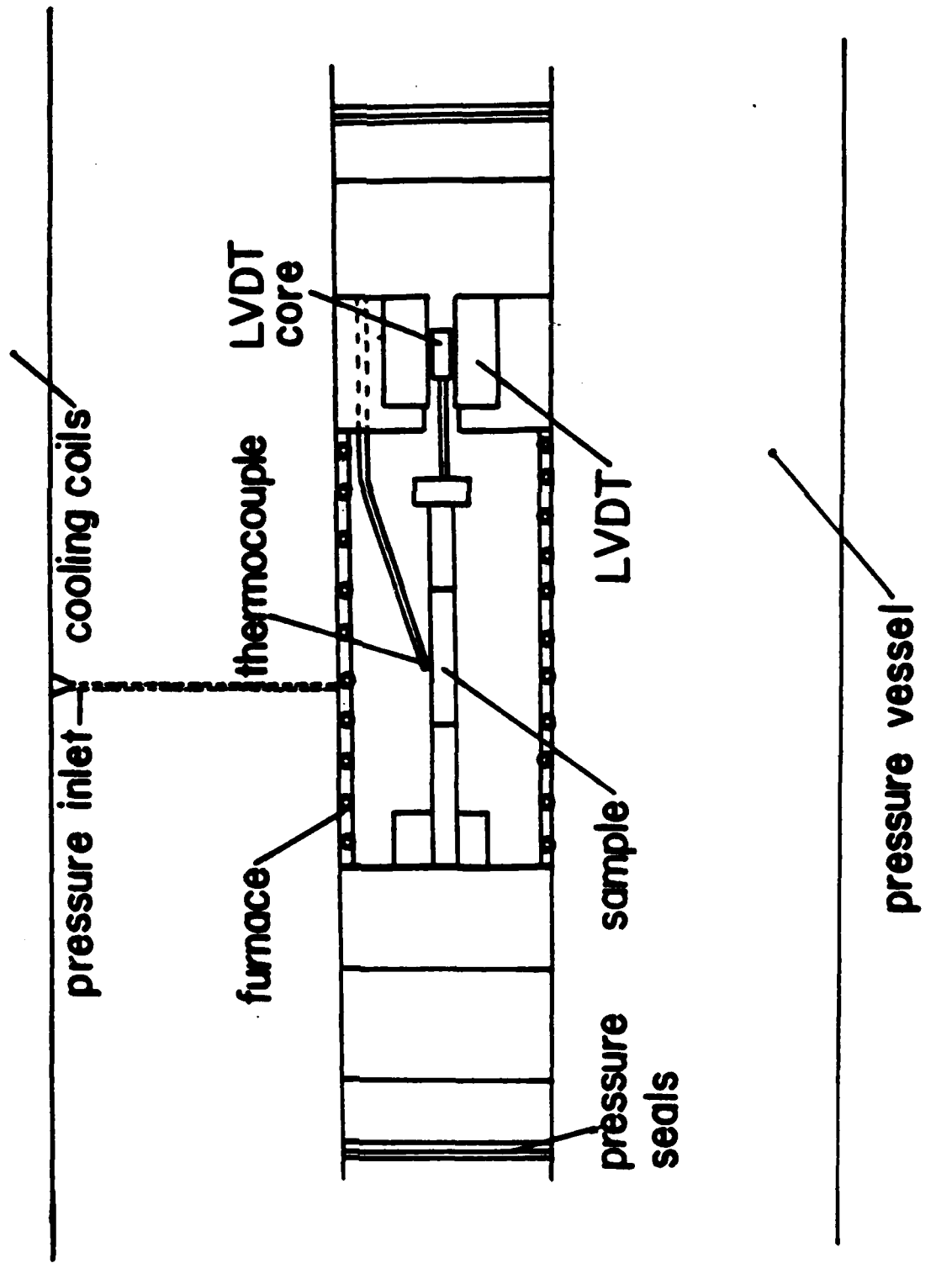
## LIST OF FIGURES

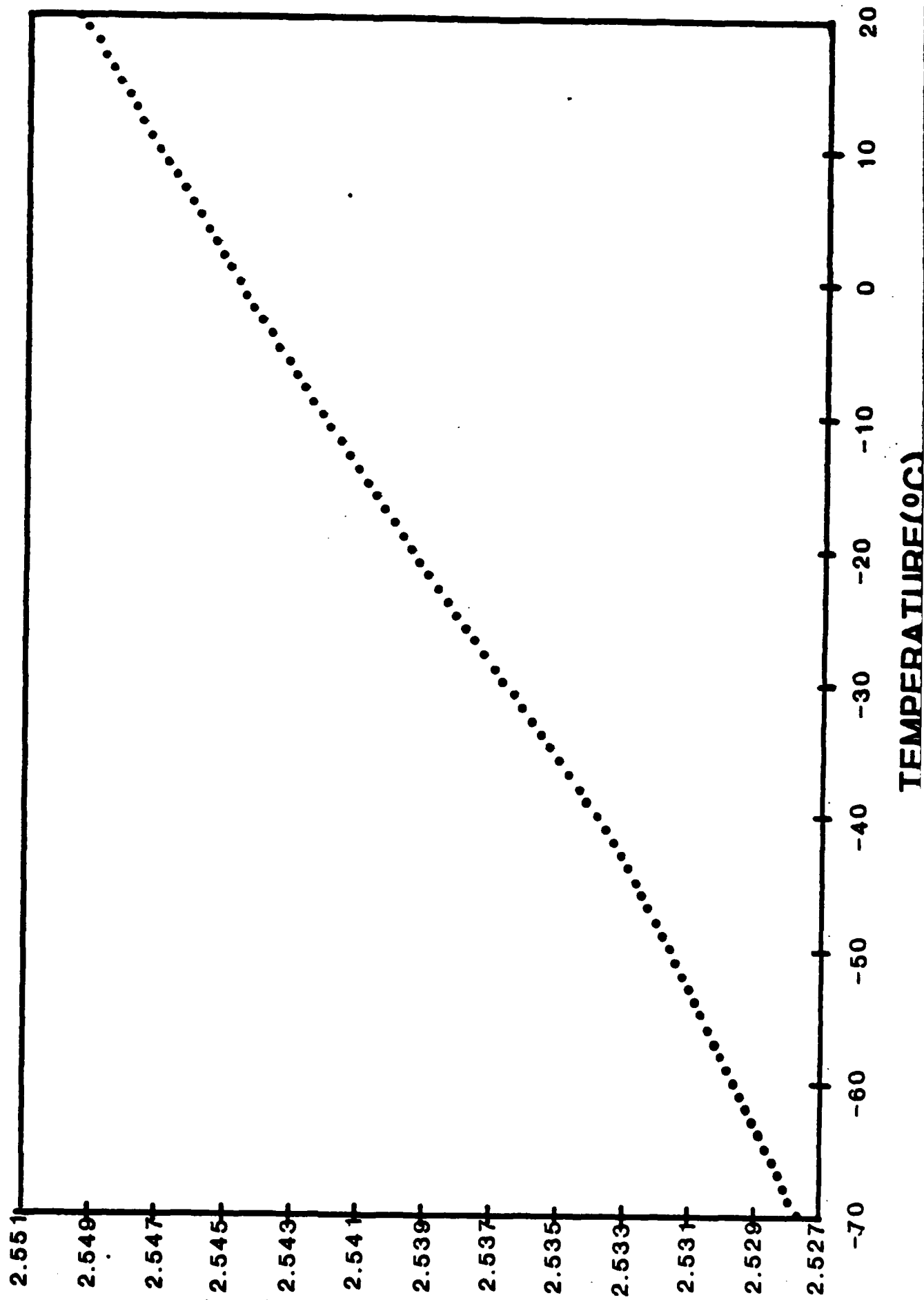
- Fig. 1 High Pressure Tension and Compression Testing Apparatus
- Fig. 2 Compressive Stress-Strain Curves of Phase II PVDF at various Pressures
- Fig. 3 Tensile Stress-Strain Curves of Phase II PVDF at various Pressures
- Fig. 4 Schematic Diagram of PVT Apparatus
- Fig. 5 Linear Dimension vs. Temperature for Unoriented Phase II PVDF
- Fig. 6 Original Samples for Tensile and Compressive Tests
- Fig. 7 Young's Modulus vs. Pressure for Phase II PVDF
- Fig. 8 Compressive and Tensile Yield Strength vs. Pressure for Phase II PVDF
- Fig. 9 Deformed Tensile and Compressive Samples Tested at 2 Kbars
- Fig. 10 Linear Dimension of Unoriented Phase I PVDF vs. Pressure
- Fig. 11 Linear Compressibility of Unoriented Phase I PVDF vs. Pressure
- Fig. 12 Linear Dimension of Unoriented Phase I PVDF vs. Temperature
- Fig. 13 Linear Thermal Expansion Coefficient of Unoriented Phase I PVDF vs. Temperature
- Fig. 14 Linear Compressibility of Unoriented and Uniaxially Oriented Phase I PVDF vs. Pressure
- Fig. 15 Volumetric Compressibility of Unoriented and Uniaxially Oriented Phase I PVDF vs. Pressure
- Fig. 16 Young's Modulus vs. Yield Strength for Phase II PVDF
- Fig. 17 The Temperature Dependence of  $\delta p$  at Various Pressures for Poled Unoriented Phase I PVDF Film
- Fig. 18 The Temperature Dependence of  $P_y$  at Various Pressures for Poled Unoriented Phase I PVDF Film
- Fig. 19 The Pressure Dependence of  $P_y$  min.,  $T_g$ , and  $\delta p$  min. for Poled Unoriented Phase I PVDF Film
- Fig. 20 The Temperature Dependence of  $\delta p$  for Uniaxially Oriented Phase I at Various Pressures
- Fig. 21 The Temperature Dependence of  $P_y$  at Various Pressure for Uniaxially Oriented Phase I PVDF Film
- Fig. 22 The Pressure Dependence of  $P_y$  min.,  $T_g$ , and  $\delta p$  min. for Uniaxially Oriented Phase I PVDF Film



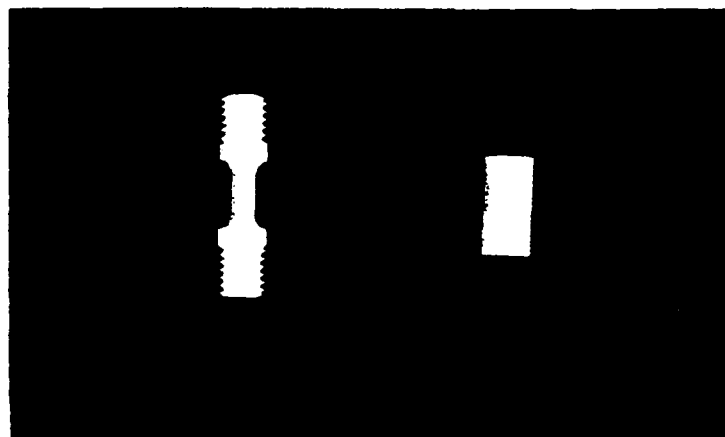


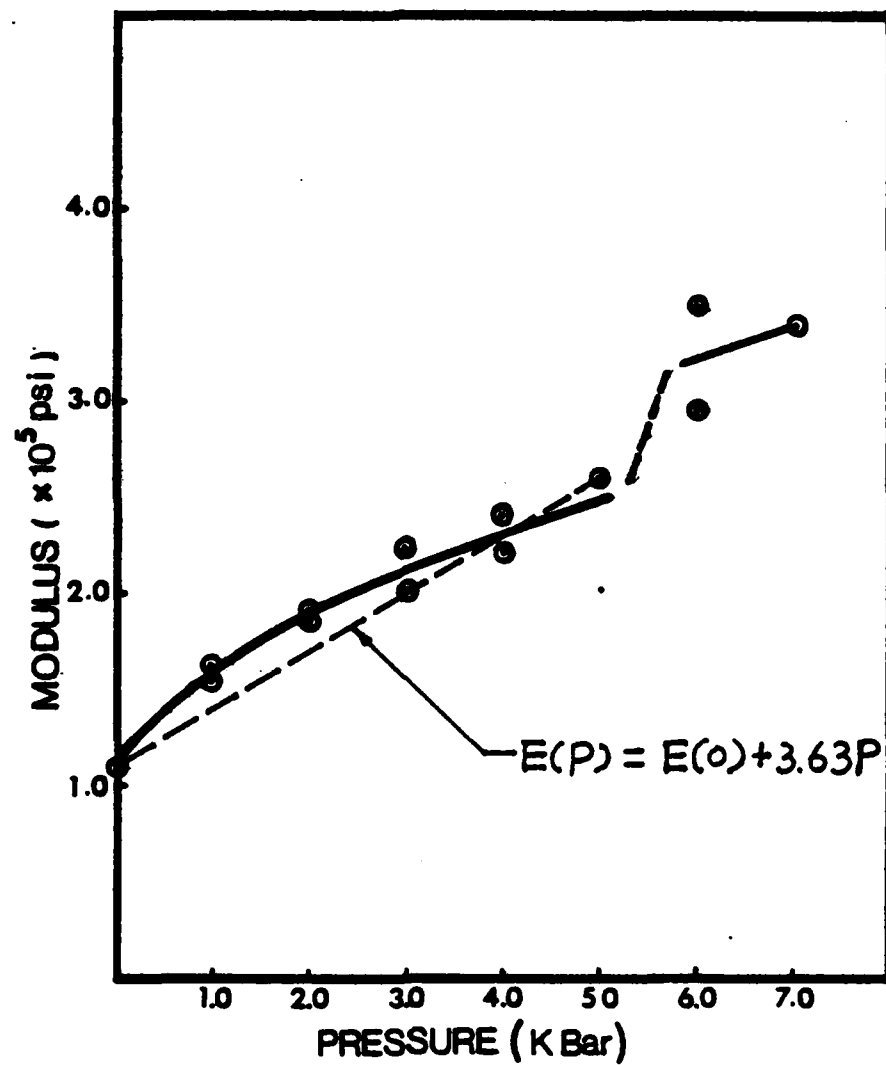


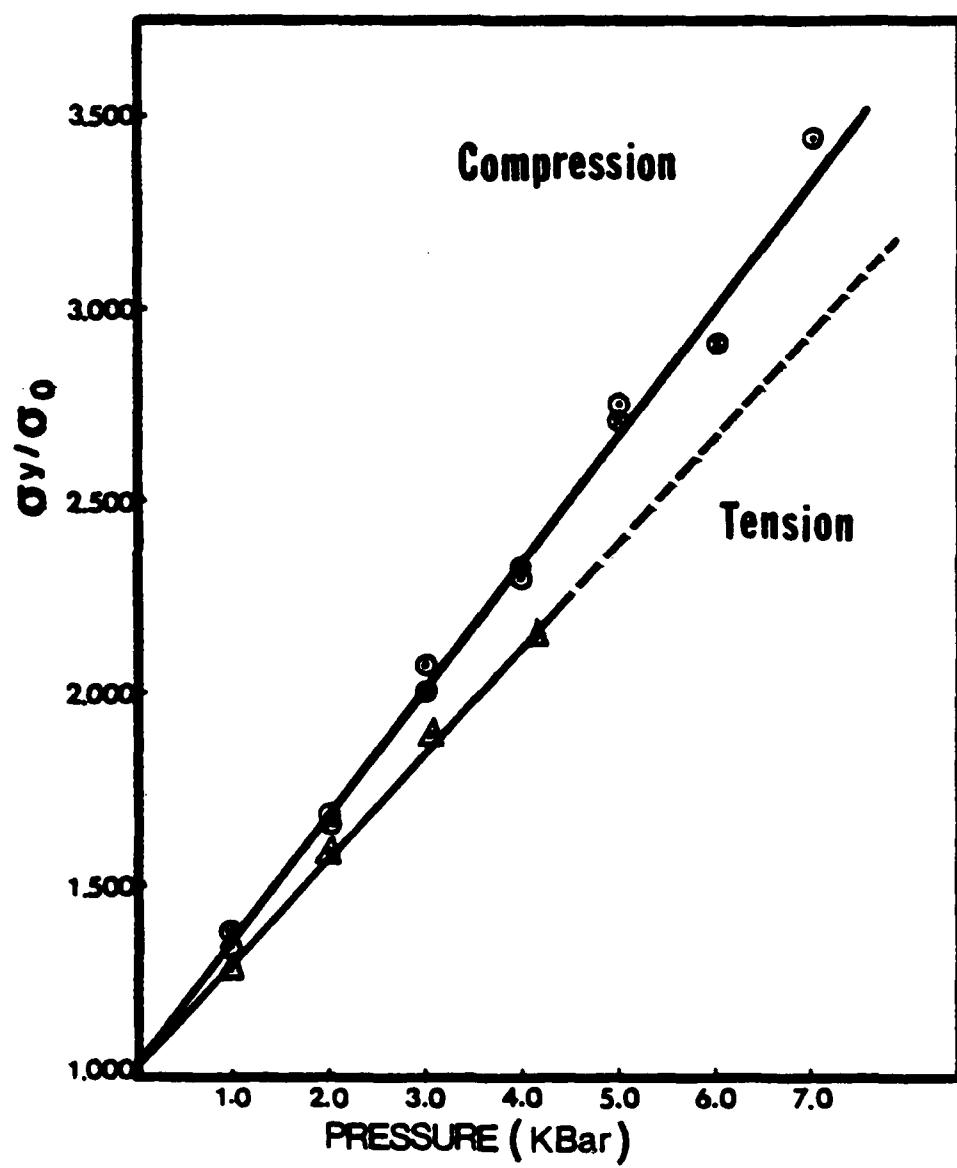


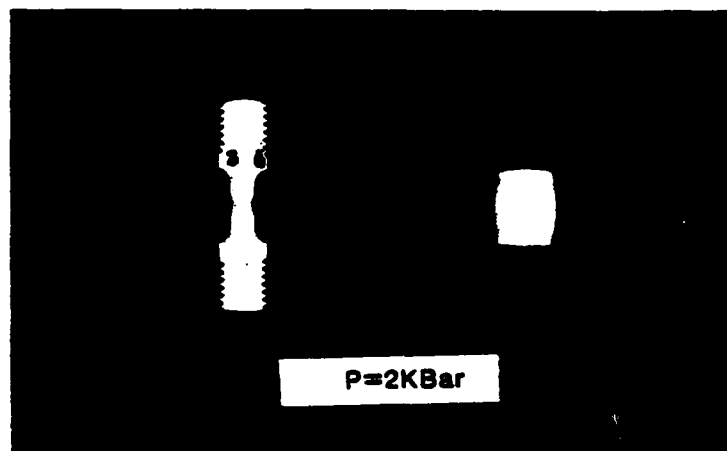


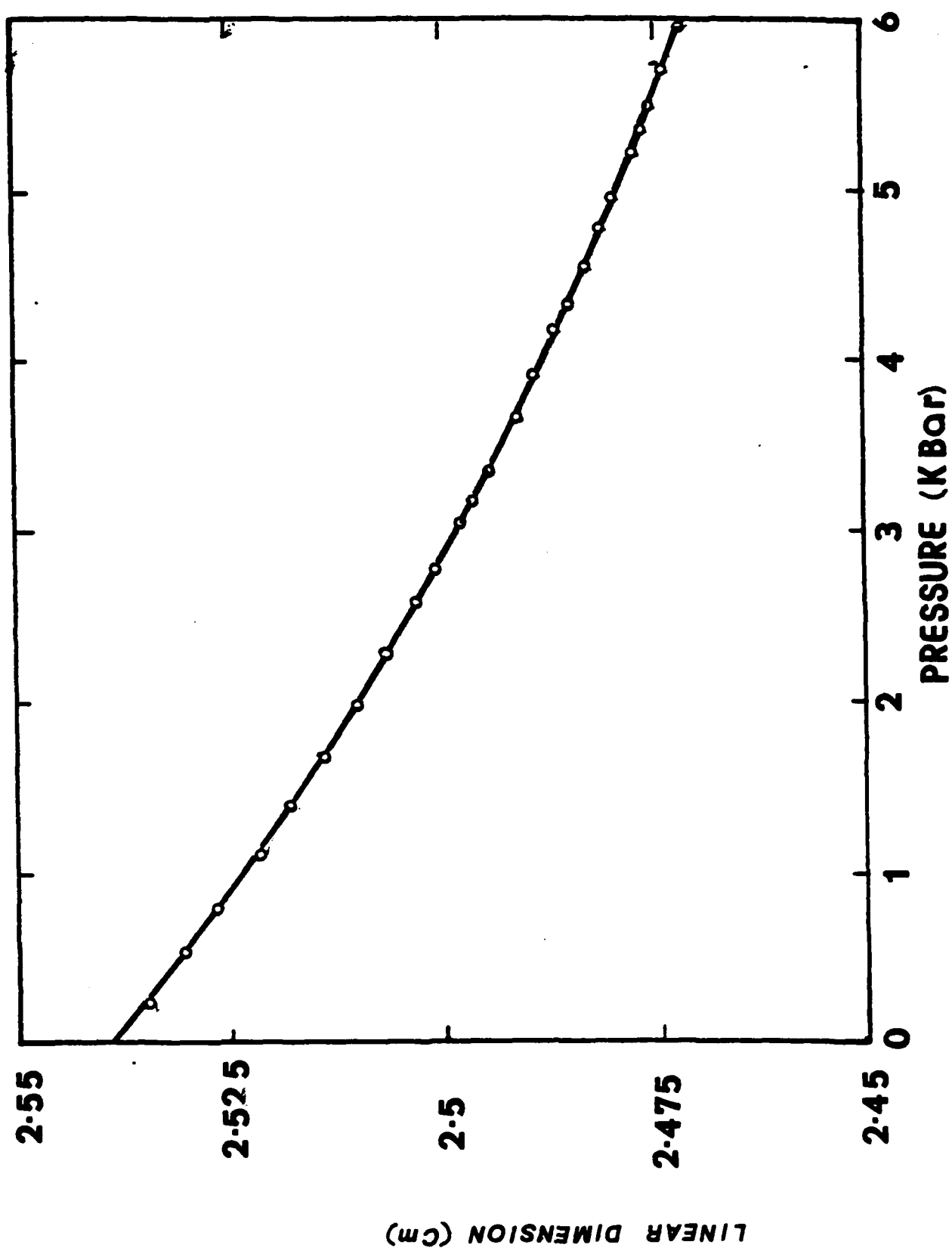


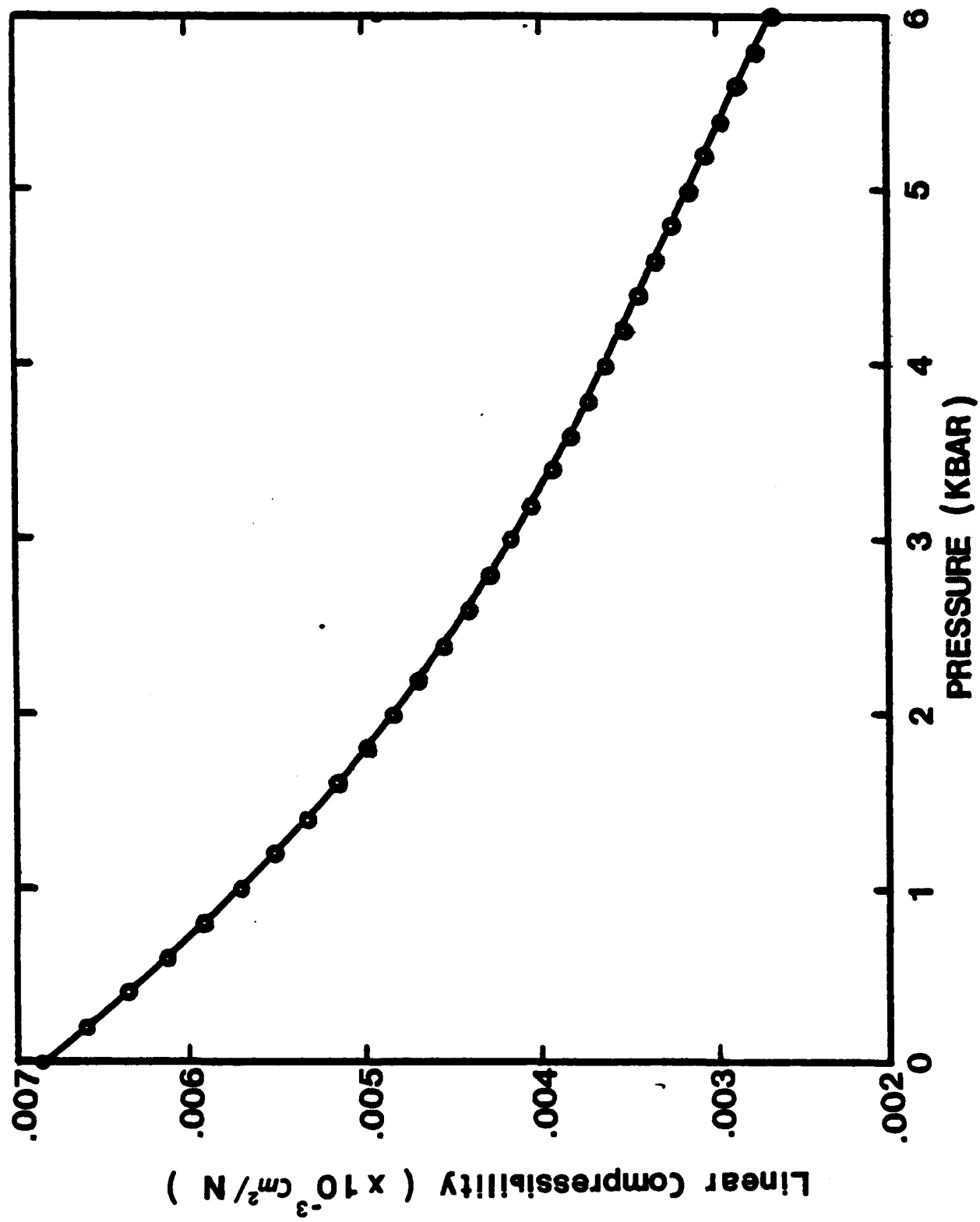


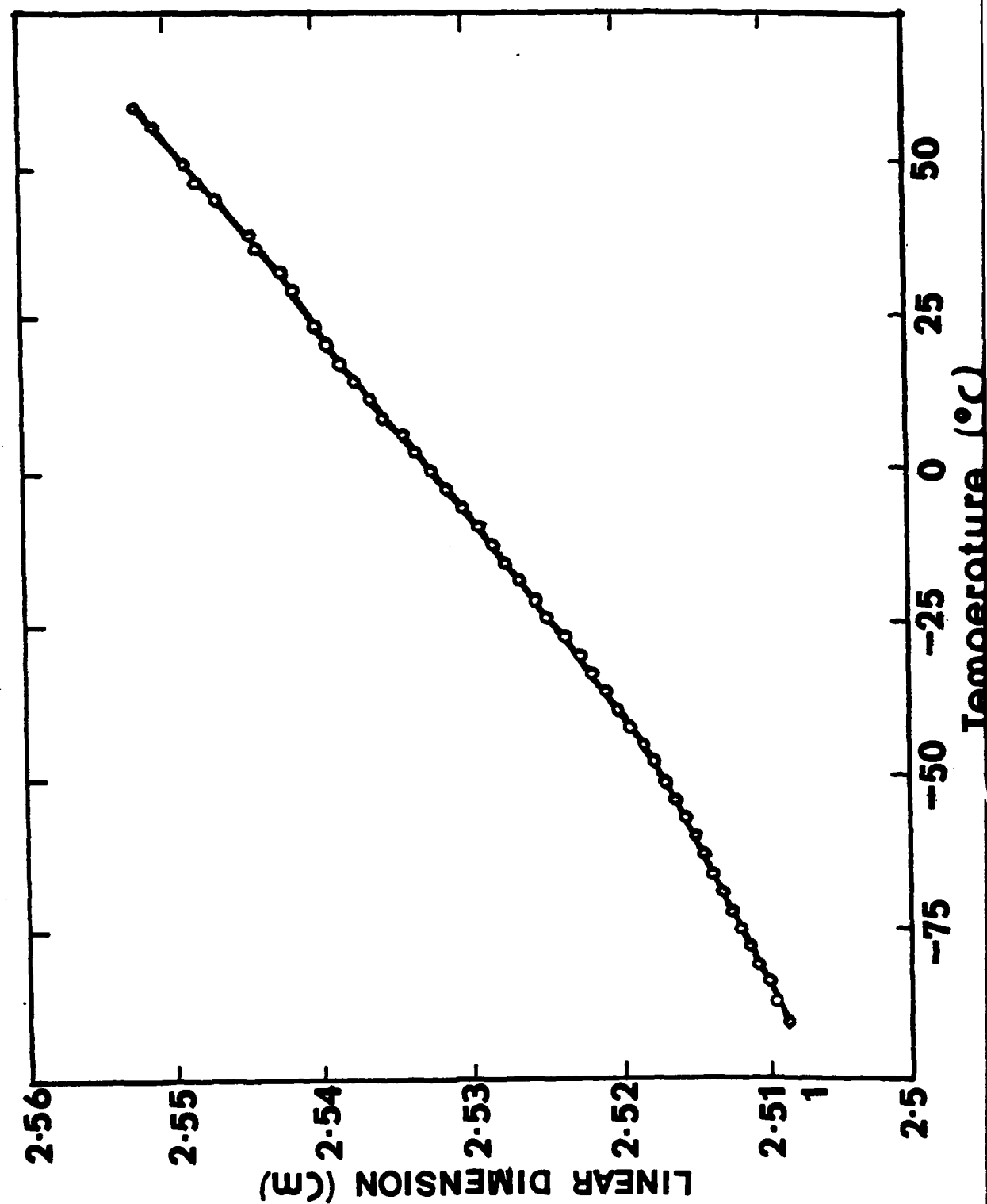


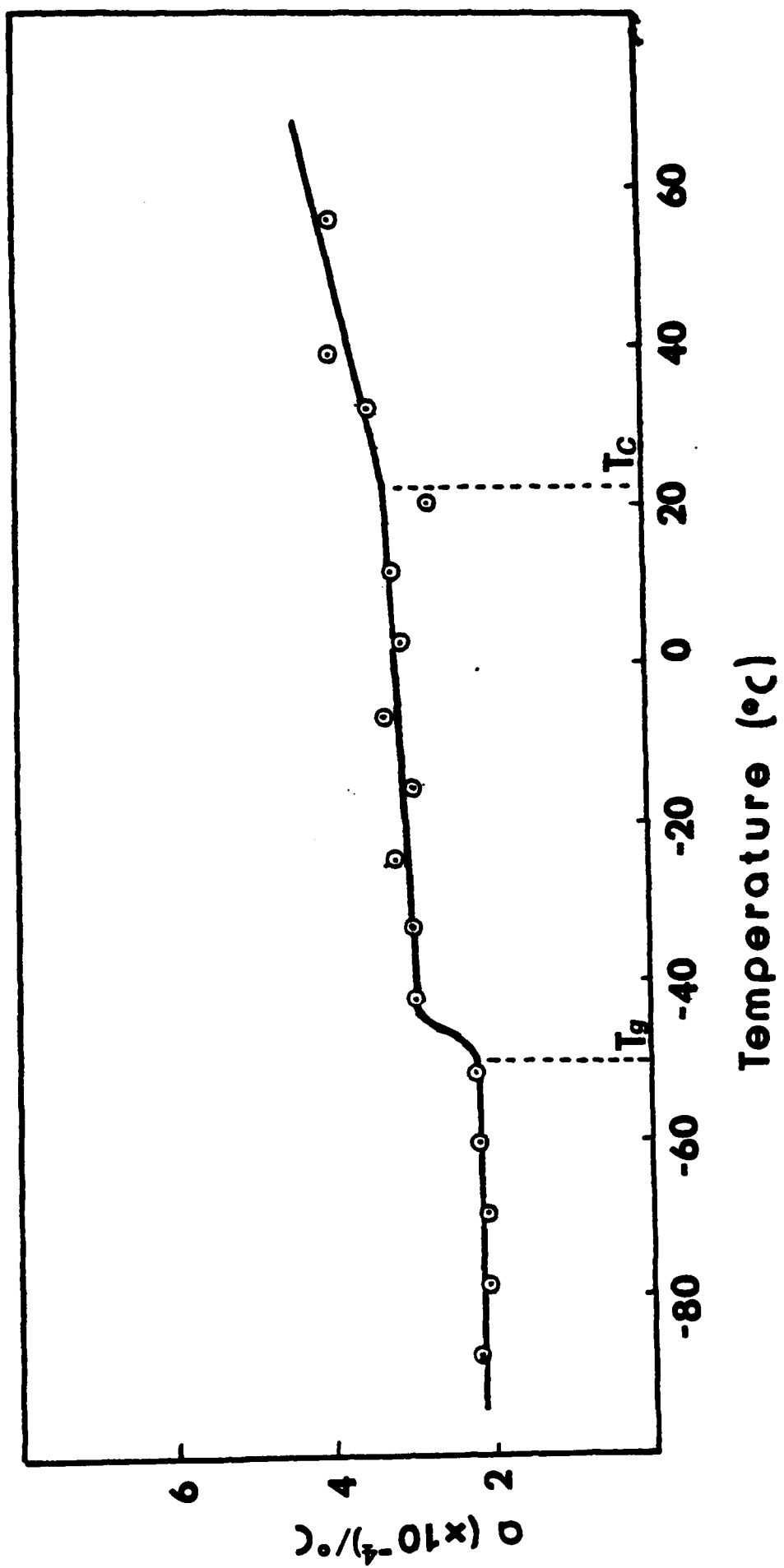




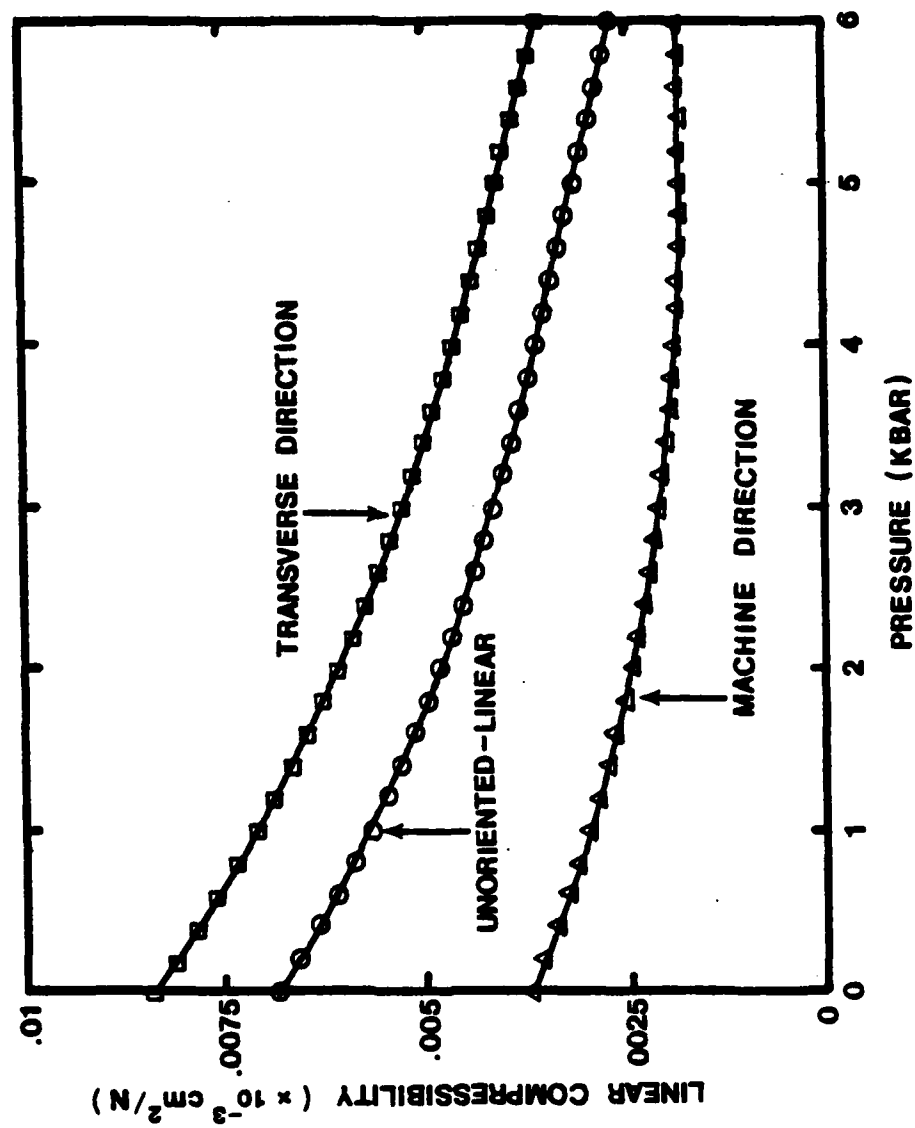


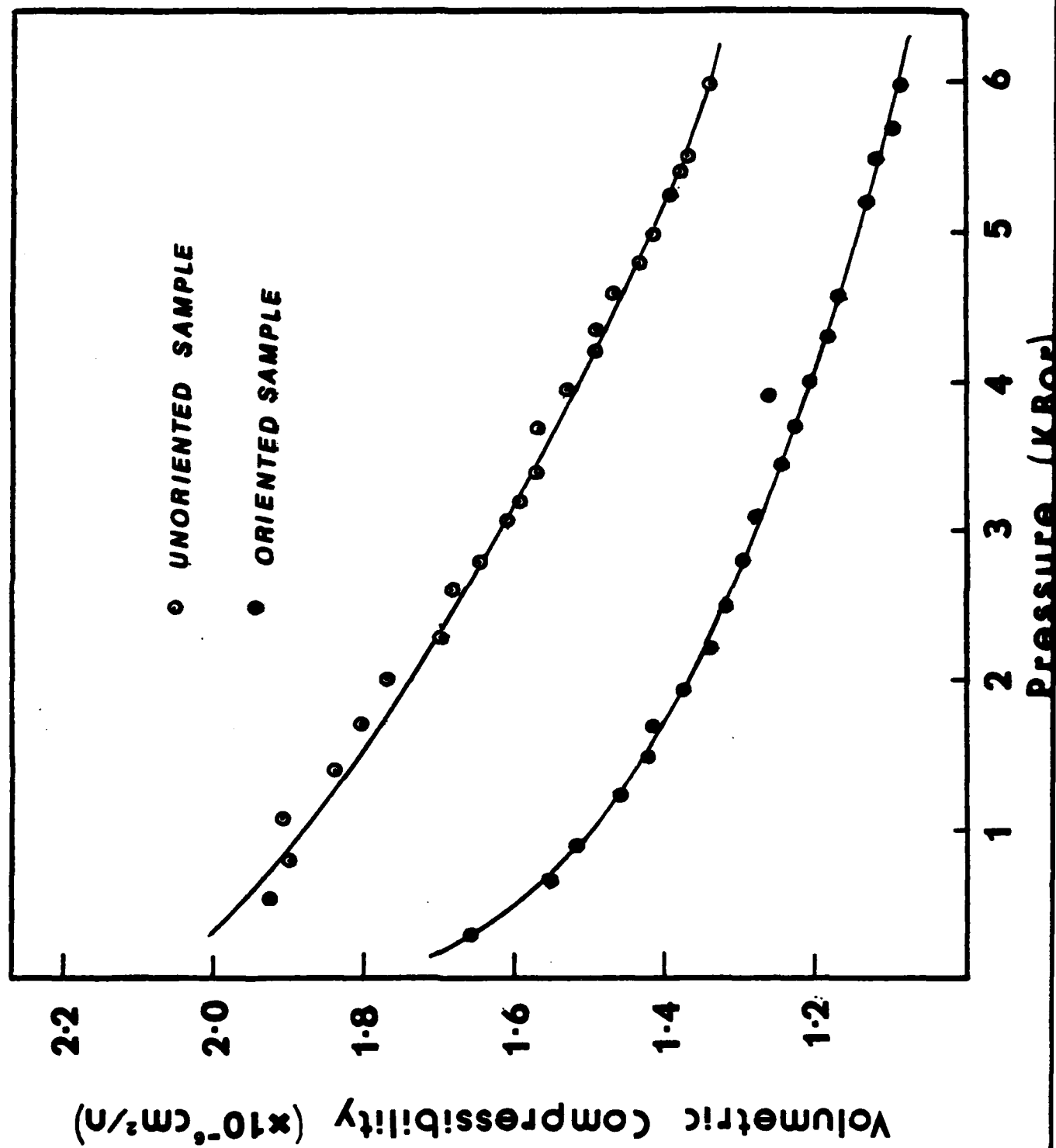


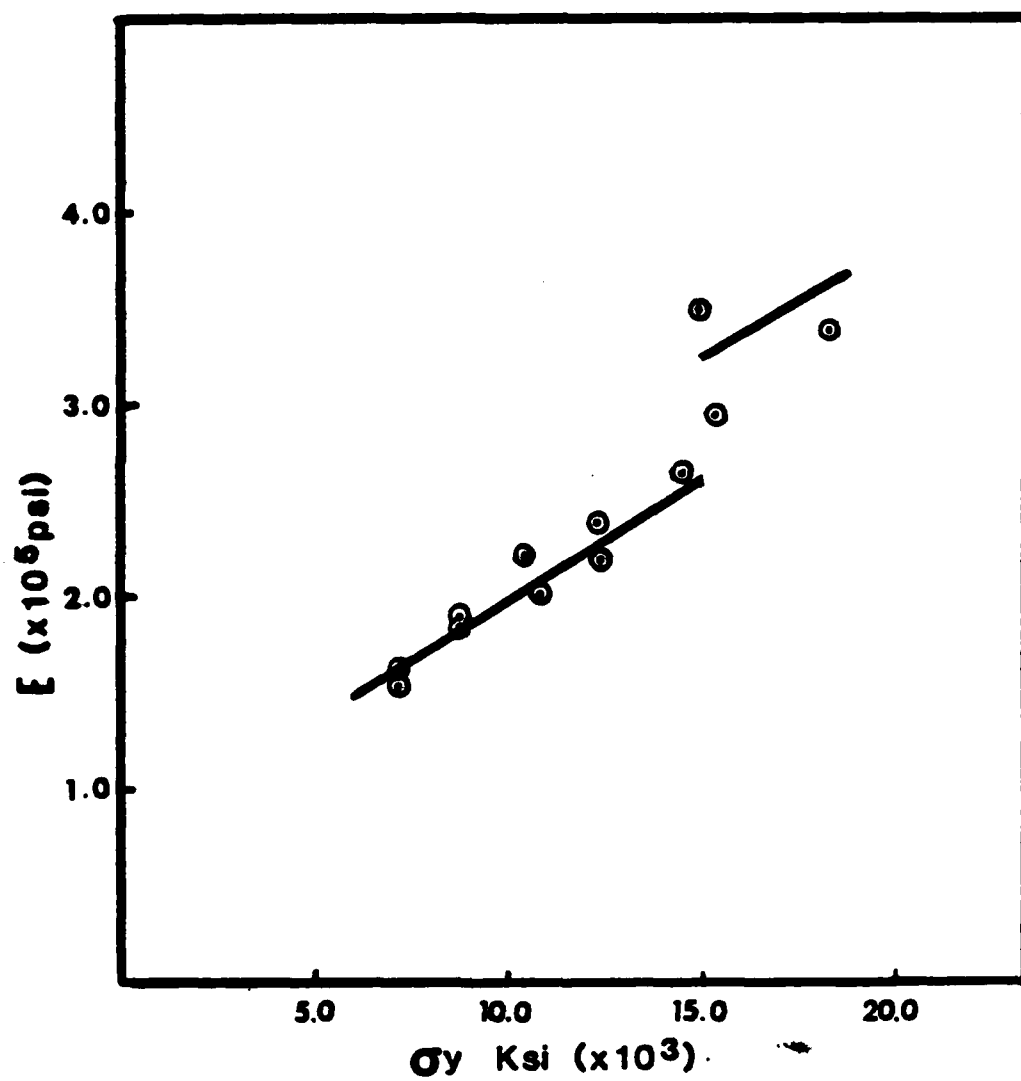


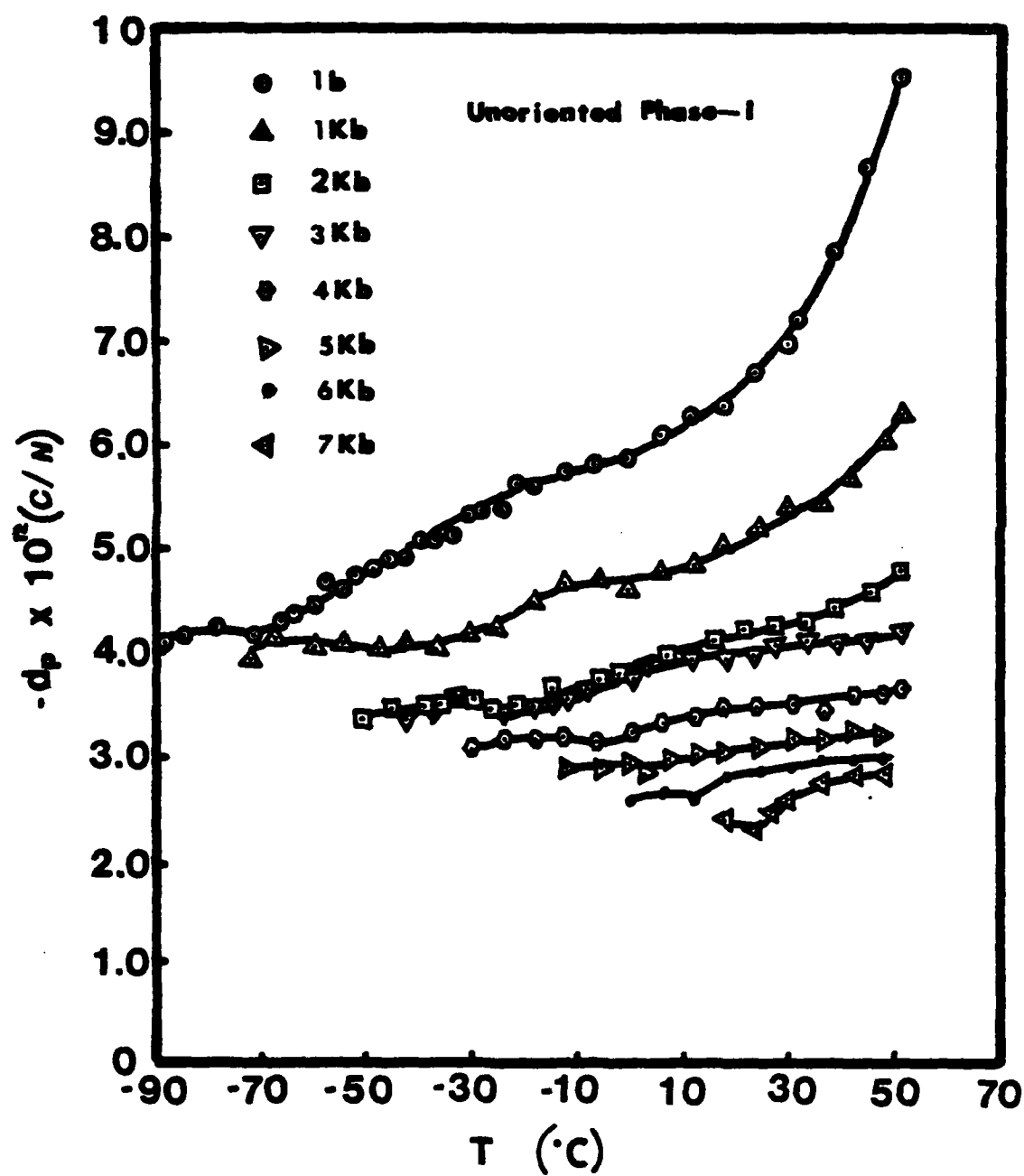


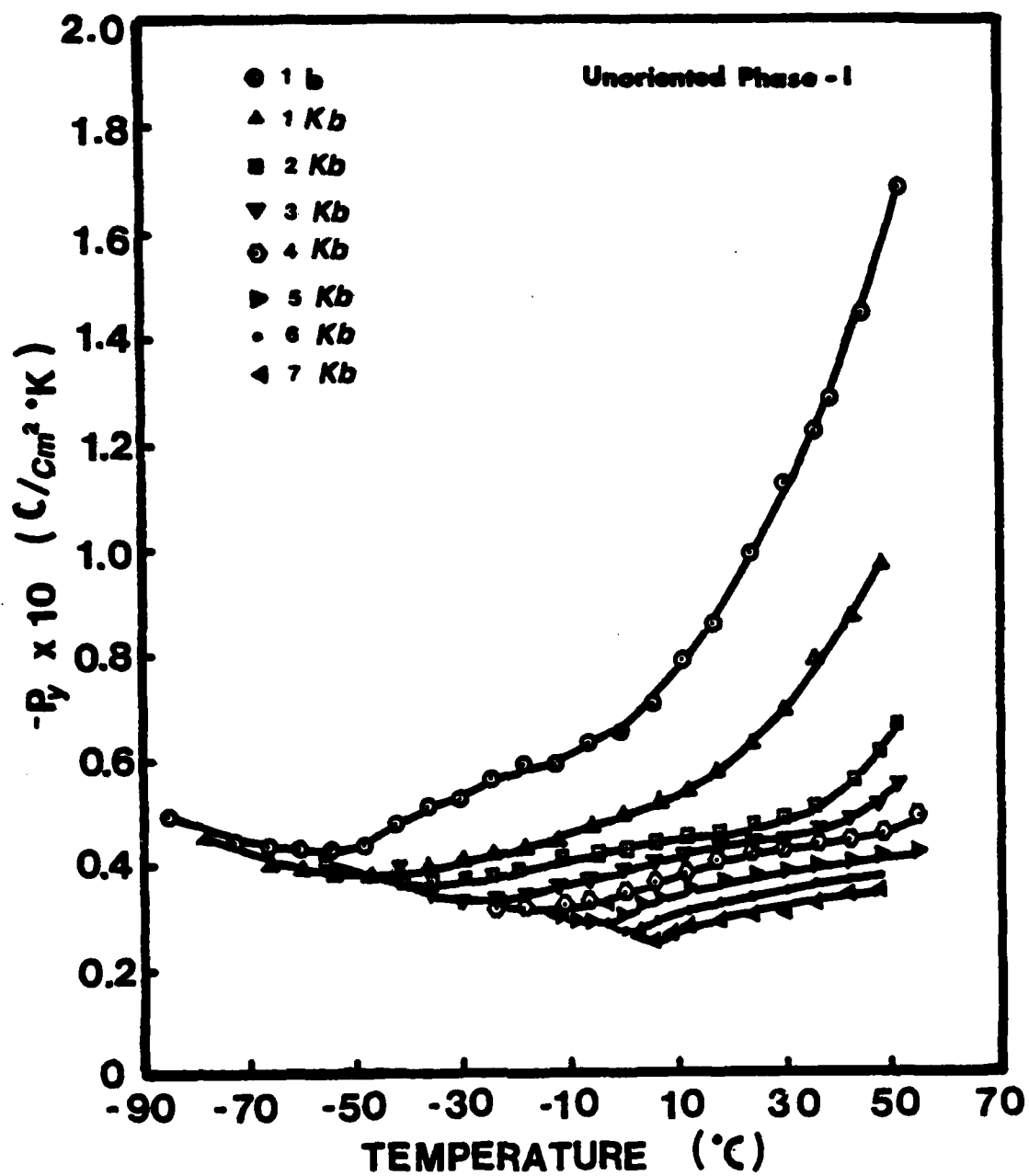


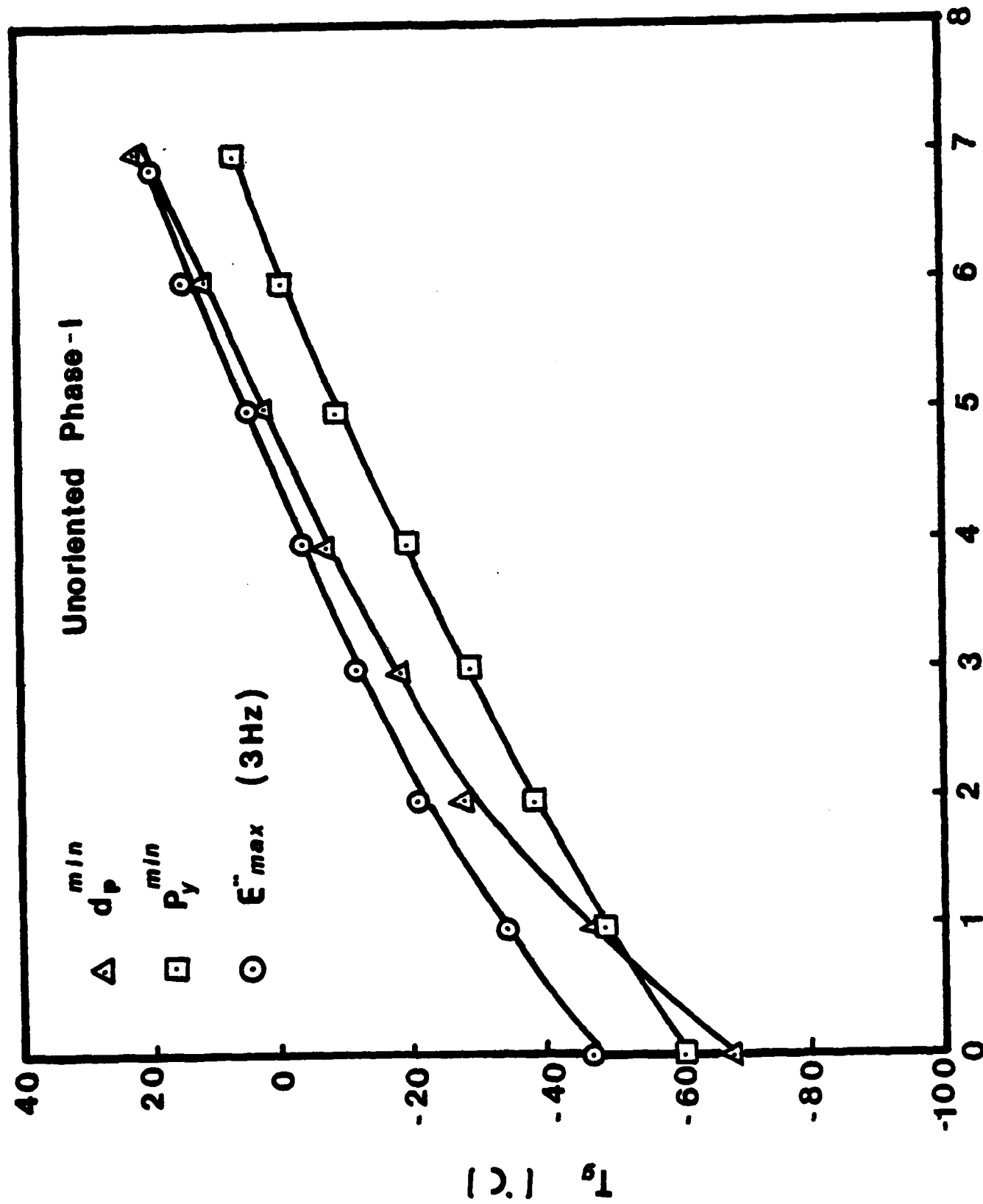


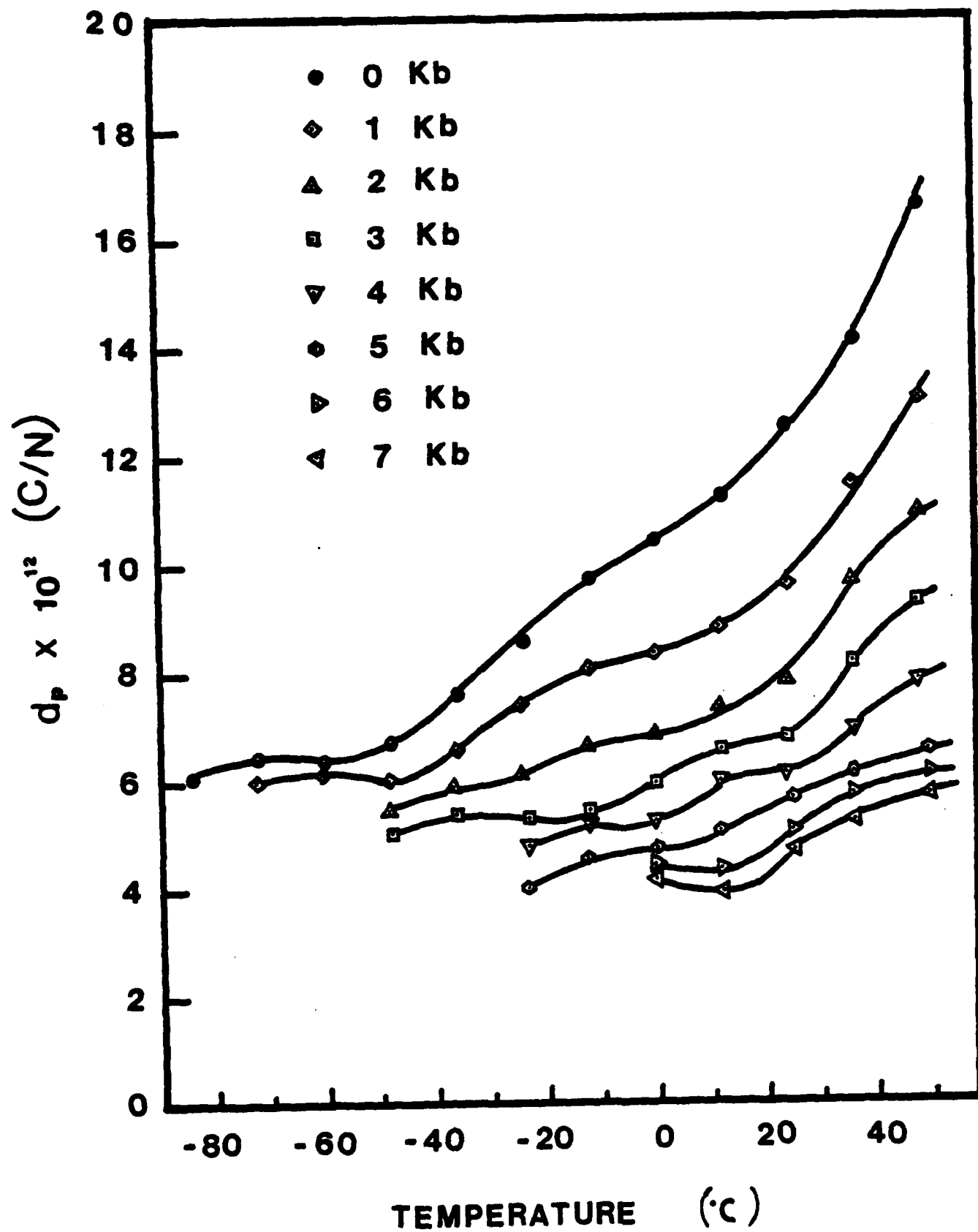


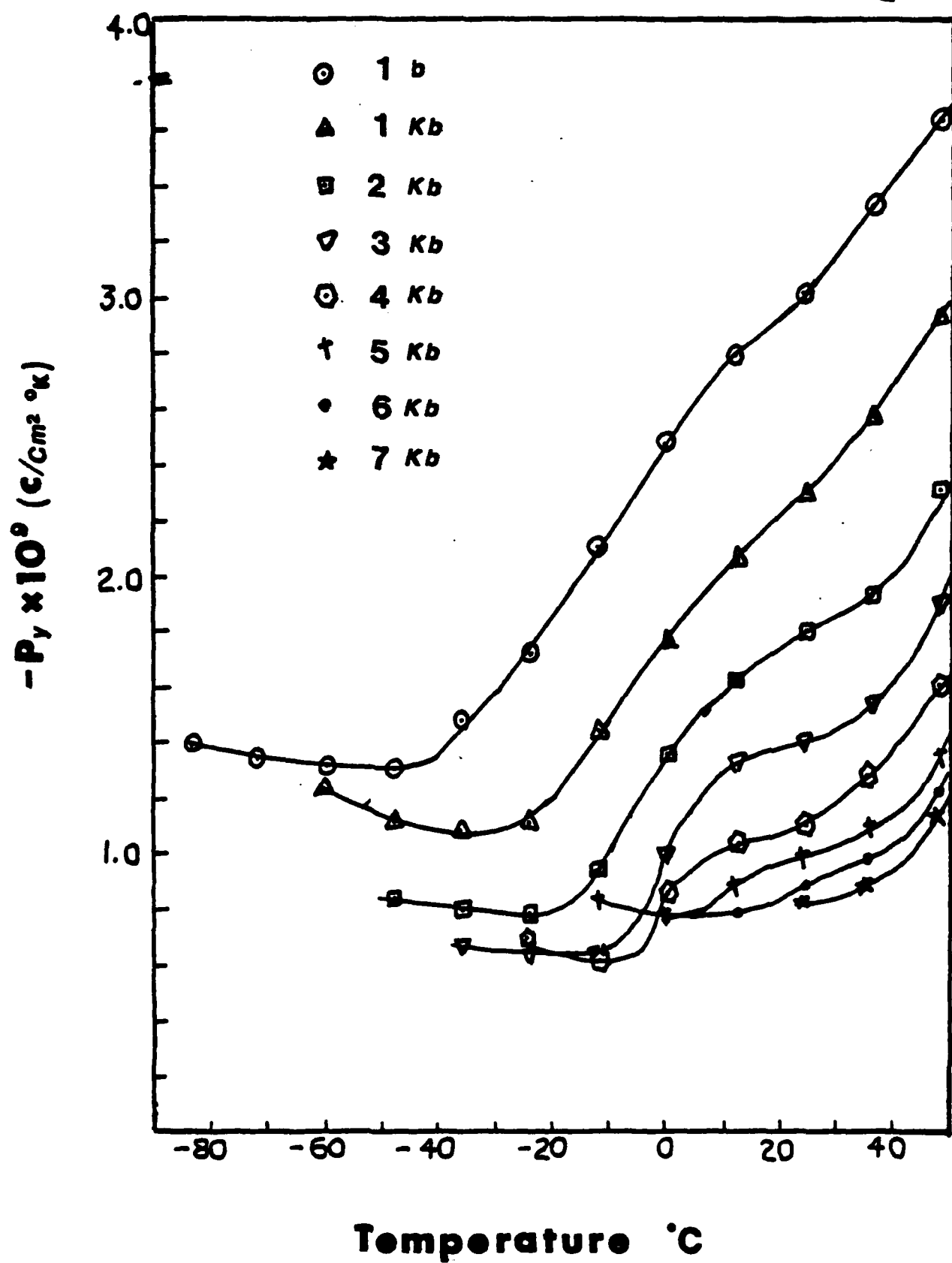




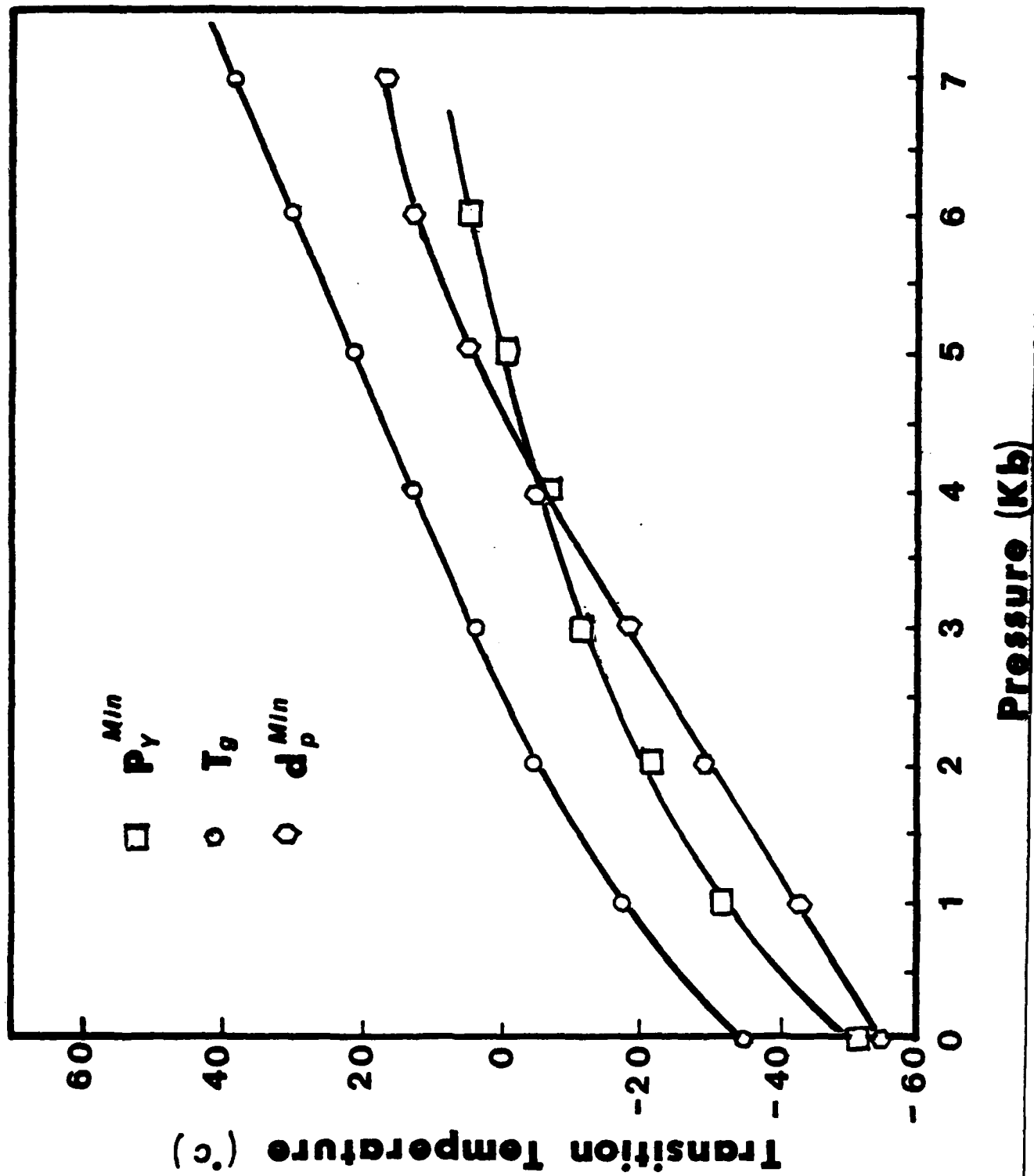












END

FILMED

3-84

DTIC